Astron. Astrophys. 362, 730–736 (2000)

ASTRONOMY AND ASTROPHYSICS

Emission lines of O III in the optical and ultraviolet spectra of planetary nebulae

F.L. Crawford[1], **F.P. Keenan**[1], **K.M. Aggarwal**[1], **A.W. Wickstead**[2], **L.H. Aller**[3], **and W.A. Feibelman**[4]

[1] The Queen's University of Belfast, Department of Pure and Applied Physics, Belfast BT7 1NN, Northern Ireland, UK (fergal.crawford@qub.ac.uk; f.keenan@qub.ac.uk; k.aggarwal@qub.ac.uk)
[2] The Queen's University of Belfast, Department of Pure Mathematics, Belfast BT7 1NN, Northern Ireland, UK (a.wickstead@qub.ac.uk)
[3] University of California, Los Angeles, CA 90024, USA (aller@bonnie.astro.ucla.edu)
[4] NASA Goddard Space Flight Center, Greenbelt, MD 20771, USA (feibelman@iue.gsfc.nasa.gov)

Received 20 June 2000 / Accepted 8 September 2000

Abstract. Recent **R**-matrix calculations of electron impact excitation rates in O III are used to calculate electron temperature and density-dependent emission line ratios
$R_1 = I(4363\,\text{Å})/I(4960\,\text{Å} + 5007\,\text{Å})$,
$R_2 = I(1661\,\text{Å} + 1667\,\text{Å})/I(4960\,\text{Å} + 5007\,\text{Å})$ and
$R_3 = I(2322\,\text{Å})/I(1661\,\text{Å} + 1667\,\text{Å})$,
for a range of electron temperatures ($7500 \le T_e \le 30\,000\,\text{K}$) and densities ($10^4 \le N_e \le 10^7\,\text{cm}^{-3}$) applicable to gaseous nebulae. The ratio-ratio diagrams (R_1, R_2) and (R_1, R_3) should, in principle, allow the simultaneous determination of T_e and N_e from measurements of the O III features in a spectrum. Plasma parameters derived for a sample of mid- to high-excitation planetary nebulae from (R_1, R_2) and (R_1, R_3) measurements, produced using a combination of ultraviolet spectra obtained with the International Ultraviolet Explorer (*IUE*) and optical data from a number of observing runs, are found to show excellent internal consistency. They also show, in general, good agreement with the values of T_e and N_e estimated from other line ratios in the nebulae, therefore providing observational support for the accuracy of the theoretical ratios and hence the atomic data adopted in their derivation.

Key words: atomic data – ISM: planetary nebulae: general

1. Introduction

Emission lines arising from transitions in O III are frequently observed in the optical (Keenan & Aggarwal 1987; McKenna et al. 1996) and ultraviolet (Clegg et al. 1987) spectra of high-excitation planetary nebulae (PNe). Under normal PNe conditions, where $N_e \le 10^5\,\text{cm}^{-3}$ (Barlow 1987), the [O III] $\lambda\lambda$ 4363, 4960 and 5007 Å transitions are in the 'coronal approximation' (Elwert 1952), so that their intensities depend almost exclusively on the magnitude of the electron impact excitation rates for the lines (Keenan & Aggarwal 1989). Therefore, the ratio $R_1 = I(4363\,\text{Å})/(I(4960\,\text{Å}{+}5007\,\text{Å})$ has traditionally been employed as an electron temperature diagnostic for the emitting plasma, since the pioneering work of Hebb & Menzel (1940). However, this early work (Menzel et al. 1941) gave values of T_e that were too low. The matter was clarified by Seaton (1953, 1954) who obtained greatly improved cross-sections. From these, new T_e estimates in the neighbourhood of 10 000 to 12 000 K (e.g., Aller 1956) have been buttressed by more recent work (see e.g., Osterbrock 1974).

However, Nussbaumer & Storey (1981) have demonstrated that the ultraviolet intercombination lines at $\lambda\lambda$ 1661 and 1667 Å and the forbidden λ 2322 Å transition, which became readily observable with the launch of the International Ultraviolet Explorer (*IUE*) satellite, should allow the simultaneous derivation of the electron temperature and density of the O III region, when combined with optical data.

In this paper we use new O III atomic data to calculate optical and ultraviolet emission line ratios in O III applicable to gaseous nebulae, and compare these with optical observations and UV spectra from the *IUE* archives. Specifically, we investigate if the O III measurements allow us to simultaneously derive reliable estimates of electron temperature and density for PNe.

2. Theoretical line ratios

The model ion for O III consisted of the 9 energetically lowest LS states, i.e. $2s^22p^2\ ^3P$, ^1D, ^1S; $2s2p^3\ ^5S$, ^3D, ^3P, ^1D, ^3S and ^1P, making a total of 15 fine-structure levels. Energies for all of these were taken from Bashkin & Stoner (1975).

Electron impact collision rates in O III were obtained from the recent **R**-matrix calculations of Aggarwal & Keenan (1999), while for Einstein A-coefficients the theoretical results of Aggarwal et al. (1997), Fleming & Brage (1997) and Froese Fischer & Saha (1985) were adopted. Proton impact excitation rates, which are only important for transitions within the $2s^22p^2\ ^3P$ ground state, were taken from Ryans et al. (1999).

Using the above atomic data in conjunction with the computer code of Dufton (1977), relative O III level populations and hence emission line strengths were derived for a range of electron temperatures and densities. Details of the procedures

Send offprint requests to: F.L. Crawford

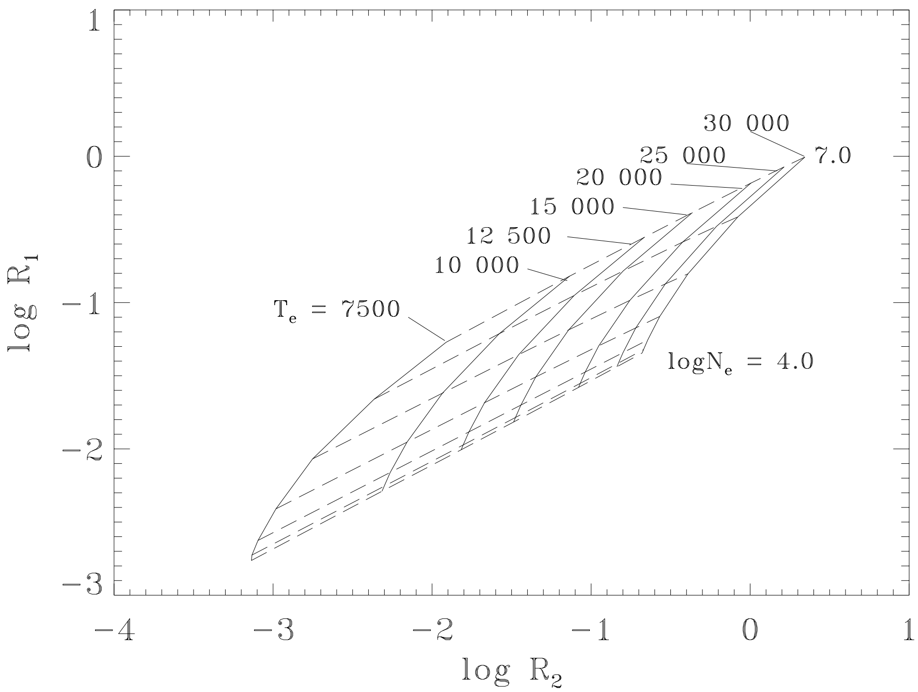

Fig. 1. Plot of the theoretical O III emission line ratio (log R_1) vs. (log R_2), where $R_1 = I(4363\,\text{Å})/I(4960\,\text{Å}{+}5007\,\text{Å})$ and $R_2 = I(1661\,\text{Å}{+}1667\,\text{Å})/I(4960\,\text{Å}{+}5007\,\text{Å})$. I is in energy units and log N_e (N_e in cm^{-3}) increases from 4.0 to 7.0 in steps of 0.5 dex. Points of constant T_e are joined by solid lines, while those of constant N_e are joined by dashed lines.

involved and approximations made may be found in Dufton (1977) and Dufton et al. (1978).

In Fig. 1 we plot (log R_1) vs. (log R_2), where

$$R_1 = \frac{I(2s^22p^2\,{}^1D - 2s^22p^2\,{}^1S)}{I(2s^22p^2\,{}^3P_{1,2} - 2s^22p^2\,{}^1D)} = \frac{I(4363\,\text{Å})}{I(4960\,\text{Å} + 5007\,\text{Å})}$$

and

$$R_2 = \frac{I(2s^22p^2\,{}^3P_{1,2} - 2s2p^3\,{}^5S_0)}{I(2s^22p^2\,{}^3P_{1,2} - 2s^22p^2\,{}^1D)} = \frac{I(1661\,\text{Å} + 1667\,\text{Å})}{I(4960\,\text{Å} + 5007\,\text{Å})}$$

for values of electron temperature $T_e = 7500 - 30\,000$ K and density $N_e = 10^4 - 10^7$ cm^{-3}.

Fig. 2 shows the plot of (log R_1) vs. (log R_3), where

$$R_3 = \frac{I(2s^22p^2\,{}^3P_1 - 2s^22p^2\,{}^1S)}{I(2s^22p^2\,{}^3P_{1,2} - 2s2p^3\,{}^5S_0)} = \frac{I(2322\,\text{Å})}{I(1661\,\text{Å} + 1667\,\text{Å})}.$$

Given uncertainties of typically $\pm$ 10 % in the adopted atomic data, we estimate that the theoretical line ratios in Figs. 1 and 2 should be accurate to approximately $\pm$ 15 %.

3. Observational data

3.1. Optical observations

Existing optical measurements of the [O III] $\lambda\lambda$ 4363, 4960 and 5007 Å forbidden transitions have been compiled for a number of nebulae. Most of the spectra were taken at the Lick Observatory, either as photographic plates or photoelectrically. Recently, all measurements have been made with the Hamilton Echelle Spectrograph at the Coudé focus of the Shane 3 m telescope. The references are listed in Table 1 and all line intensities are listed in Table 2.

3.2. IUE observations

For each nebula we chose two high resolution *IUE* spectra (where available), one short wavelength and one long wavelength, from the *IUE* archive at Villafranca in Spain. These exposures were all taken using the large ($10'' \times 23''$) aperture on the *IUE* and are listed in Table 1. The O III $\lambda\lambda$ 1661, 1667 and 2322 Å emission line fluxes have been measured from these exposures using the spectrum analysis program DIPSO (Howarth et al. 1996). Good quality, high dispersion *IUE* images could not be found for CD–23, but Aller et al. (1981) list the ratios R_1 and R_2 for this object. We did not search for *IUE* spectra of NGC 6818, as line intensities for this object are listed by Hyung et al. (1999).

In Table 2 we list the UV and optical line intensities for each nebula, relative to H$\beta = 100$. These intensities have been corrected for interstellar extinction using the extinction curve of Seaton (1979) in conjunction with the logarithmic extinction at Hβ, $C = 1.47E(B-V) = \log\,[I(\text{H}\beta)/F(\text{H}\beta)]$, where $I(\text{H}\beta)$ and $F(\text{H}\beta)$ are the intrinsic and observed Hβ line intensities respectively. Values of C are listed in Table 2 and have been derived through a comparison of the theoretical He II 1640 Å/4686 Å and hydrogen recombination line ratios (e.g., Hummer & Storey 1987) with those measured from optical and/or *IUE* observations of our PNe (for details, see Feibelman et al. 1996).

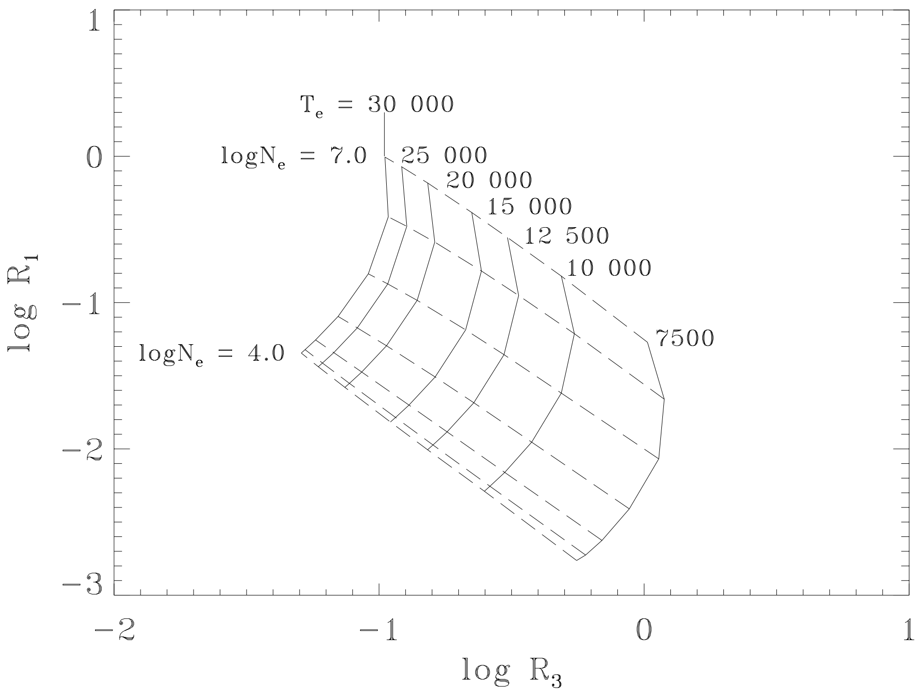

Fig. 2. Plot of the theoretical O III emission line ratio (log R_1) vs. (log R_3), where $R_1 = I(4363\,\text{Å})/I(4960\,\text{Å}+5007\,\text{Å})$ and $R_3 = I(2322\,\text{Å})/I(1661\,\text{Å}+1667\,\text{Å})$. As before, log N_e (N_e in cm^{-3}) increases from 4.0 to 7.0 in steps of 0.5 dex. Points of constant T_e are joined by solid lines, while those of constant N_e are joined by dashed lines.

Table 1. Summary of optical and *IUE* observations.

Object	Optical Measurement Reference	*IUE* Image Number[1]
CD–23	Aller et al. (1981)	–
IC 2165	Hyung (1994)	SWP 07964, LWR 06936
IC 3568	Lee et al. (1969)	SWP 14868
NGC 2440	Hyung & Aller (1998)	SWP 07263
NGC 3242	Barker (1985)	SWP 15289, LWR 12705
NGC 6210	Aller et al. (1970)	SWP 10732, LWR 14149
NGC 6572	Hyung et al. (1994)	SWP 42059, LWP 20789
NGC 6818	Hyung et al. (1999)	–
NGC 7027	Keyes et al. (1990)	SWP 04716
NGC 7662	Hyung & Aller (1997)	SWP 04106, LWR 06805

[1] R_1 and R_2 are given for CD–23 by Aller et al. (1981), while Hyung et al. (1999) list O III line strengths for NGC 6818 (see text).

Table 2. O III emission line intensities, corrected for interstellar extinction and relative to H$\beta = 100$.

Object	$I(1661)$	I(1667)	$I(2322)$	$I(4363)$	$I(4960)$	$I(5007)$	C^1
CD–23[2]	–	–	–	18.7	473	1390	0.36
IC 2165	14.0	34.9	90.1	20.8	370	1158	0.68
IC 3568	3.32	5.37	–	13.8	359	1069	0.32 (a)
NGC 2440	19.9	39.0	–	26.8	515	1585	0.53
NGC 3242	13.8	29.9	9.32	12.5	399	1230	0.09 (a)
NGC 6210	2.01	7.20	3.03	6.20	377	1051	0.14 (b)
NGC 6572	2.12	5.32	2.46	8.90	364	1077	0.40
NGC 6818[3]	8.45	23.4	5.56	23.4	780	2511	0.30
NGC 7027	10.8	19.0	–	17.6	512	1553	1.37
NGC 7662	47.5	99.2	25.7	15.7	369	1224	0.10

[1] The values listed here for $C = 1.47E(B-V)$ (see text) are found in the optical measurement reference, unless otherwise noted: (a) Feibelman (1982); (b) Cahn & Kaler (1971).
[2] Aller et al. (1981) list these optical intensities uncorrected for interstellar extinction, but they give corrected values for R_1 and R_2.
[3] Line intensities for NGC 6818 are given by Hyung et al. (1999).

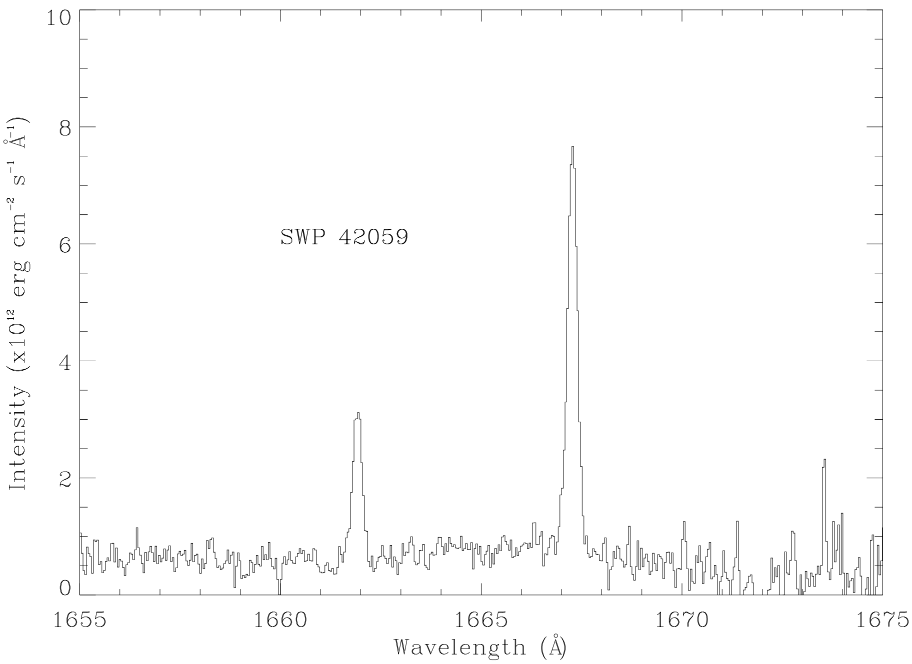

Fig. 3. High resolution *IUE* exposure SWP 42059 of NGC 6572 in the wavelength range $1655 - 1675$ Å, illustrating the O III] lines at $\lambda\lambda$ 1661 and 1667 Å.

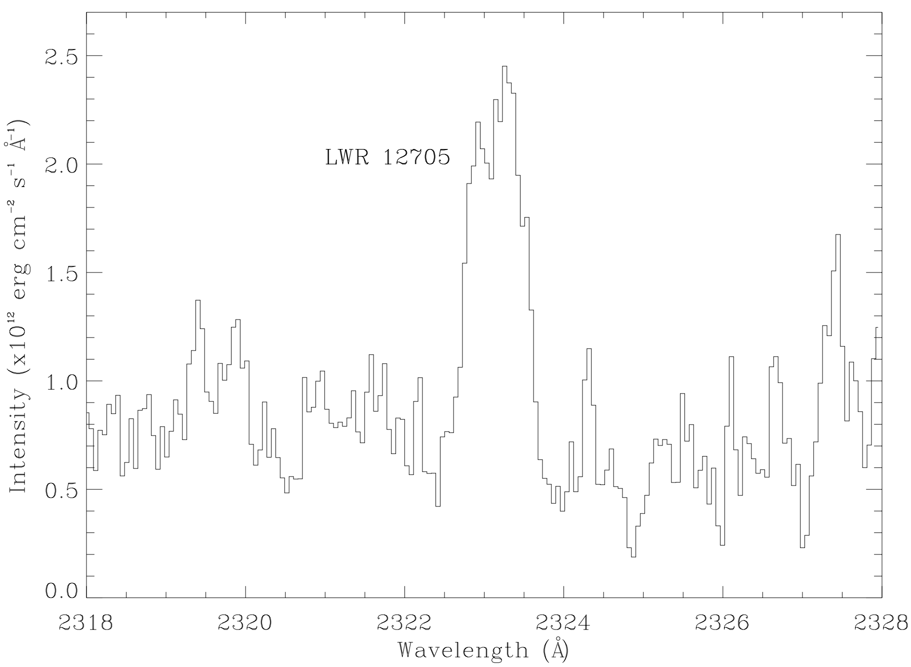

Fig. 4. High resolution *IUE* exposure LWR 12705 of NGC 3242 in the wavelength range $2318 - 2328$ Å, illustrating the [O III] line at λ 2322 Å.

To illustrate the quality of the *IUE* spectra, we plot in Figs. 3 and 4 sections of the high resolution exposures of NGC 6572 in the wavelength range $1655 - 1675$ Å and NGC 3242 in the wavelength range $2318 - 2328$ Å, respectively. The O III] intercombination lines at $\lambda\lambda$ 1661 and 1667 Å and the [O III] forbidden line at λ 2322 Å are clearly visible in these spectra.

3.3. Line ratios and estimated accuracies

The observed values of R_1, R_2 and R_3 derived from Table 2 are listed in Table 3. We estimate that the uncertainties in the optical line intensities should be approximately $\pm$ 10 %, implying that the optical ratio R_1 should be accurate to typically $\pm$ 15 %. However, the accuracy in general of the UV line intensities in the *IUE* images will be lower than this, around $\pm$ 20 %. Hence the observed R_2 and R_3 ratios are probably only reliable to $\pm$ 25 %.

4. Results and discussion

In Table 4 we summarise the electron temperatures and logarithmic electron densities (T_e, log N_e), derived from measurements of (R_1, R_2) and (R_1, R_3) in conjunction with the theoretical results in Figs. 1 and 2, respectively, along with their mean values

Table 3. Emission line ratios.

Object	R_1 $\frac{I(4363\,Å)}{I(4960\,Å+5007\,Å)}$	R_2 $\frac{I(1661\,Å+1667\,Å)}{I(4960\,Å+5007\,Å)}$	R_3 $\frac{I(2322\,Å)}{I(1661\,Å+1667\,Å)}$
CD–23	$1.13-2$[1]	$2.04-2$	–
IC 2165	$1.36-2$	$3.19-2$	$1.85-0$
IC 3568	$9.66-3$	$6.09-3$	–
NGC 2440	$1.28-2$	$2.80-2$	–
NGC 3242	$7.67-3$	$2.69-2$	$2.13-1$
NGC 6210	$4.34-3$	$6.45-3$	$3.29-1$
NGC 6572	$6.18-3$	$5.16-3$	$3.31-1$
NGC 6818	$7.10-3$	$9.68-3$	$1.75-1$
NGC 7027	$8.52-3$	$1.92-2$	–
NGC 7662	$9.85-3$	$9.21-2$	$1.75-1$

[1] $A-B$ implies $A\times10^{-B}$.

Table 4. Derived [O III] electron temperatures and densities.

Object	(T_e, log N_e) (R_1, R_2)	(T_e, log N_e) (R_1, R_3)	(T_e, log N_e)$_{mean}$	(T_e, log N_e)$_{other}$[1]
CD–23	13 000, 4.0	–	13 000, 4.0	13 200, 3.2
IC 2165	15 000, 4.0	I[2]	15 000, 4.0	13 000, 3.7
IC 3568	9500, 5.4	–	9500, 5.4	12 400, 2.9
NGC 2440	14 000, 4.0	–	14 000, 4.0	13 500, 3.7
NGC 3242	I	11 000, 4.7	11 000, 4.7	11 400, 3.9
NGC 6210	I	9000, 4.5	9000, 4.5	10 000, 4.1
NGC 6572	10 000, 4.8	9500, 5.0	9750, 4.9	11 000, 4.7
NGC 6818	11 500, 4.0	11 500, 4.0	11 500, 4.0	11 400, 3.7
NGC 7027	13 500, 4.0	–	13 500, 4.0	14 000, 4.4
NGC 7662	11 500, 4.9	12 000, 4.5	11 750, 4.7	12 100, 3.7

[1] From the optical measurement reference, listed in Table 1.
[2] Indicates that (T_e, log N_e) are indeterminate owing to the observed line ratios lying outside the grid of values in Fig. 1 or 2.

(T_e, log N_e)$_{mean}$. We also list plasma parameters, denoted (T_e, log N_e)$_{other}$, found for our objects by other studies using different ions which have similar ionisation potentials and therefore spatial distributions to O III, such as $I(4711\,Å)/I(4740\,Å)$ and $I(7238\,Å)/I(4711+4740\,Å)$ in Ar IV (Keenan et al. 1997).

It can be seen from Table 4 that plasma parameters could not be derived from (R_1, R_2) for NGC 3242 and NGC 6210 and, for IC 2165, T_e and N_e could not be obtained from (R_1, R_3). This is because the measured ratios for these PNe were found to lie outside the grids plotted in Figs. 1 and 2. For NGC 3242 and 6210, this may be due to the fact that the optical data employed came from observations which are of lower quality than those obtained with the Hamilton Echelle Spectrograph. NGC 6210 was observed using photographic plates supplemented with data from Oke's photoelectric scanner at Mount Wilson (Aller et al. 1970), while the resolution of the NGC 3242 observations was limited to about 10 Å FWHM (Barker 1985). We also note that the largest discrepancy between (T_e, log N_e)$_{mean}$ and (T_e, log N_e)$_{other}$ occurs for IC 3568, where the observational techniques employed were similar to those for NGC 6210 (Lee et al. 1969). However, this does not explain why we were unable to obtain plasma parameters from both (R_1, R_2) and (R_1, R_3) for IC 2165.

The three PNe (NGC 6572, 6818 and 7662) for which we were able to derive values of T_e and log N_e from both (R_1, R_2) and (R_1, R_3) show extremely good internal consistency, with T_e and log N_e differing on average by only 330 K and 0.2 dex, respectively. Furthermore, we find our results to be in good agreement with those determined from other line ratios, with discrepancies in T_e averaging less than 850 K. With reference to Sect. 3.3, it can be seen that our derived electron temperatures should be in error by about ± 1000 K at T_e = 10 000 K and ± 3000 K at T_e = 15 000 K, meaning that all our measurements are in excellent agreement with those from other studies. These results provide good observational support for the accuracy of the theoretical O III line ratio diagnostics, and hence the atomic data used in their derivation.

Our values of log N_e are generally in good agreement with those derived from other diagnostics, with the exceptions of IC 3568, NGC 3242 and NGC 7662. In the first two of these cases the resolution of the optical spectra was low, as described above, and so the errors in measuring the O III line strengths were more pronounced. In the case of NGC 7662 it should be noted that, within errors, we can easily reconcile our measurement of log N_e with the comparison value quoted in Table 4. We also note

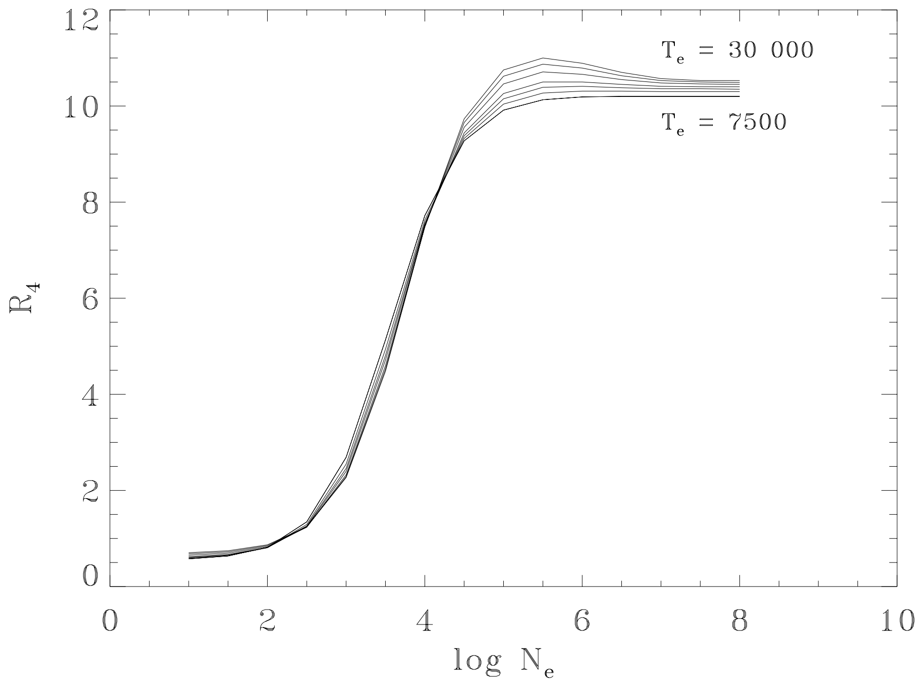

Fig. 5. Plot of the theoretical O III emission line ratio R_4 vs. log N_e, where $R_4 = I(52\,\mu\mathrm{m})/I(88\,\mu\mathrm{m})$. I is in energy units and N_e is in cm^{-3}.

that densities given as log $N_e = 4.0$ could be over-estimated due to bunching of the diagnostics at densities lower than this (see Figs. 1 and 2).

Hyung et al. (1999) found that T_e tends to be low for low-excitation ions and high for high-excitation ions. For example, in their study of NGC 6818, they derived $T_e \sim 9500$ K for [N II] and $T_e \sim 13\,000$ K for [Cl IV]. However, Keenan et al. (1999) found an [O II] electron temperature for NGC 6818 of $T_e = 19\,000$ K, while Keenan et al. (1997), found an [Ar IV] electron temperature of $T_e = 16\,000$ K. Liller & Aller (1954) found that high-excitation nebulae tend, in general, to have higher T_e than their low-excitation counterparts, but the correlation was weak. We find that PNe with a higher excitation class demonstrate a higher [O III] electron temperature – IC 3568, NGC 6210 and NGC 6572 are all medium-excitation nebulae and all have derived temperatures below 10 000 K, whereas the other PNe under investigation are all high-excitation nebulae and all have derived temperatures above 11 000 K.

Over the last few decades, standard formulae have been employed for the derivation of electron temperatures and densities from the R_1 line ratio, the coefficients of which have slowly evolved as the atomic parameters have improved. We were unable to fit our data to a formula of the form used by Kaler (1986), as our theoretical line ratios have been derived from a complete solution of the statistical equilibrium equation for a 15 level model ion, rather than from a simplification of the p^2 equilibrium solution (Seaton 1960). Hence, using *Mathematica* (Wolfram 1996) and the methods described in Keenan et al. (1997), we have produced an expression to directly estimate plasma parameters from R_1. We note that the function used to estimate (T_e, $\log N_e$) from R_1 is too extensive to reproduce here. However it is available from one of the authors (a.wickstead@qub.ac.uk) on request.

Finally, in Fig. 5 we plot the IR ratio, R_4, against log N_e, where

$$R_4 = \frac{I(2s^2 2p^2\,{}^3P_2 - 2s^2 2p^2\,{}^3P_1)}{I(2s^2 2p^2\,{}^3P_1 - 2s^2 2p^2\,{}^3P_0)} = \frac{I(52\,\mu\mathrm{m})}{I(88\,\mu\mathrm{m})}$$

We note that R_4 is density dependent over the range $N_e = 10^2 - 10^5\mathrm{cm}^{-3}$, but shows very little variation with temperature. However, this ratio neglects any effects due to the Bowen mechanism, in which a He II resonance line photoexcites a wavelength-incident transition (Bhatia & Kastner 1987). In our case, Bowen pumping can significantly deplete the $2p^2\ {}^3P_2$ level in O III, which is the upper level of the 52μm line. As can be seen from Fig. 2 of Bhatia & Kastner, this could lead to the underestimation of electron density by more than an order of magnitude for high excitation nebulae.

Acknowledgements. FLC holds a research studentship from the Department of Education for Northern Ireland, while KMA is grateful to EPSRC for financial support. This research was supported by National Science Foundation Grant Nos. AST 90-14133, AST 93-13991, and AST 94-16985, and Space Telescope Science Institute Grant No. AR–06372.01–95A, to the University of California, Los Angeles. We also gratefully acknowledge the support provided by NATO travel grant CRG.930722. This research has made use of NASA's Astrophysics Data System Abstract Service.

References

Aggarwal K.M., Hibbert A., Keenan, F.P., 1997, ApJS 108, 393
Aggarwal K.M., Keenan F.P., 1999, ApJS 123, 311
Aller L.H., 1956, Gaseous Nebulae. Wiley, New York
Aller L.H., Czyzak S.J., Buerger E.G., 1970, ApJ 162, 783
Aller L.H., Keyes C.D., Czyzak S.J., 1981, ApJ 250, 596

Barker T., 1985, ApJ 294, 193
Barlow M.J., 1987, MNRAS 227, 161
Bashkin S., Stoner J.O., 1975, Atomic Energy Levels and Grotrian Diagrams. North-Holland, Amsterdam, p. 176
Bhatia A.K., Kastner S.O., 1987, Phys. Scripta 35, 778
Cahn J.H., Kaler J.B., 1971, ApJS 22, 319
Clegg R.E.S., Harrington J.P., Barlow M.J., Walsh J.R., 1987, ApJ 314, 551
Dufton P.L., 1977, Comput. Phys. Commun. 13, 25
Dufton P.L., Berrington K.A., Burke P.G., Kingston A.E., 1978, A&A 62, 111
Elwert G., 1952, Z. Naturforsch 7A, 432
Feibelman W.A., 1982, AJ 87, 555
Feibelman W.A., Hyung S., Aller L.H., 1996, MNRAS 278, 625
Fleming J., Brage T., 1997, J. Phys. B 30, 1385
Froese Fischer C., Saha H.P., 1985, Phys. Scripta 32, 181
Hebb M.H., Menzel D.H., 1940, ApJ 92, 408
Howarth I.D., Murray J., Mills D., Berry D.S., 1996, DIPSO (V3.4), Starlink User Note No. 50, 20
Hummer D.G., Storey P.J., 1987, MNRAS 224, 801
Hyung S., 1994, ApJS 90, 119
Hyung S., Aller L.H., 1997, ApJ 491, 242
Hyung S., Aller L.H., 1998, PASP 110, 466
Hyung S., Aller L.H., Feibelman, W.A., 1994, MNRAS 269, 975
Hyung S., Aller L.H., Feibelman W.A., 1999, ApJ 514, 878
Kaler J.B., 1986, ApJ 308, 322
Keenan F.P., Aggarwal K.M., 1987, ApJ 319, 403
Keenan F.P., Aggarwal K.M., 1989, JA&A 10, 147
Keenan F.P., Aller L.H., Bell K.L., et al., 1999, MNRAS 304, 27
Keenan F.P., McKenna F.C., Bell K.L., et al., 1997, ApJ 487, 457
Keyes C.D., Aller L.H., Feibelman W.A., 1990, PASP 102, 59
Lee P., Aller L.H., Czyzak S.J., Duvall R.N., 1969, ApJ 155, 853
Liller W., Aller, L.H., 1954, ApJ 120, 48
McKenna F.C., Keenan F.P., Kaler J.B., et al., 1996, PASP 108, 610
Menzel D.H., Aller L.H., Hebb M.H., 1941, ApJ 93, 230
Nussbaumer H., Storey P.J., 1981, A&A 99, 177
Osterbrock D.E., 1974, Astrophysics of Gaseous Nebulae. Freeman, San Francisco
Ryans R.S.I., Foster-Woods V.J., Reid R.H.G., Keenan F.P., 1999, A&A 345, 663
Seaton M.J., 1953, PRS A218, 401
Seaton M.J., 1954, MNRAS 114, 154
Seaton M.J., 1960, R. P. Ph. 23, 313
Seaton M.J., 1979, MNRAS 187, 73P
Wolfram S., 1996, The Mathematica Book. Cambridge University Press, Cambridge